Accuracy of Finite-Difference Harmonic Frequencies in Density Functional Theory

Kuan-Yu Liu, Jie Liu,* and John M. Herbert

Analytic Hessians are often viewed as essential for the calculation of accurate harmonic frequencies, but the implementation of analytic second derivatives is nontrivial and solution of the requisite coupled-perturbed equations engenders a sizable memory footprint for large systems, given that these equations are not required for energy and gradient calculations in density functional theory. Here, we benchmark the alternative approach to harmonic frequencies based on finite differences of analytic first derivatives, a procedure that is amenable to large-scale parallelization. Not only for absolute frequencies but also for isotopic and conformer-dependent frequency shifts in flexible molecules, we find that the finite-difference approach exhibits mean errors < 0.1 cm^{-1} as compared to results based on an analytic Hessian. For very small frequencies corresponding to nonbonded vibrations in noncovalent complexes (for which the harmonic approximation is questionable anyway), the finite-difference error can be larger, but even in these cases the errors can be reduced below 0.1 cm^{-1} by judicious choice of the displacement step size and a higher-order finite-difference approach. The surprising accuracy and robustness of the finite-difference results suggests that availability of the analytic Hessian is not so important in today's era of commodity processors that are readily available in large numbers. © 2017 Wiley Periodicals, Inc.

DOI: 10.1002/jcc.24811

Introduction

In quantum chemistry, analysis of harmonic vibrational frequencies provides important information about the stability of structures located via geometry optimization and serves as a first point of contact with vibrational spectroscopy. The conventional wisdom has long held that the "proper" (and most accurate) way to compute harmonic frequencies is to derive and implement analytic second derivatives of the energy with respect to displacements of the nuclei, that is, the analytic Hessian. This exercise is nontrivial, however, even at the level of density functional theory (DFT), to which we limit the following discussion. Calculation of the analytic Hessian requires second functional derivatives $\delta^2 E_{xc}/\delta\rho^2$ whereas energy and gradient calculations require only first derivatives, $\delta E_{xc}/\delta\rho$. Solution of so-called coupled-perturbed equations is also required,[1] engendering a memory footprint of $\mathcal{O}(N_{basis}^2 N_{atoms})$. Although this footprint can be split into segments across batches of atoms,[2] reducing the memory requirement by a factor of $N_{atoms}/N_{segments}$, two-electron integrals must be recomputed for each segment. Derivation and implementation of analytic Hessians for correlated wave function methods is even more involved.

The finite-difference (FD) approach, in contrast, is simple and parallelizes trivially, with different displacements performed on different processors and without the need (at the DFT level) to solve memory-intensive coupled-perturbed equations. This is potentially important in situations where a large number of processors are available but come with severe limits on wall time, a configuration that is often encountered at supercomputer centers. In addition, to the best of our knowledge the analytic Hessian of the VV10 nonlocal correlation functional[3] has yet to be implemented in any quantum chemistry software, meaning that analytic Hessians are unavailable for several very promising new functionals such as ωB97X-V,[4] B97M-V,[5] and ωB97M-V.[6]

Historically, FD results have been viewed as inferior in quality to analytic Hessian results, and in some quantum chemistry applications this may indeed be the case. In this study, we set out to quantify the extent to which the FD approach can be trusted for harmonic vibrational frequencies computed using DFT. Not only are the absolute vibrational frequencies of interest, but also isotope- and conformer-dependent frequency shifts, as these are often the relevant observables in experimental vibrational spectroscopy.

Computational Details

Calculations were performed using the B3LYP, B3LYP-D3,[7] and ωB97X-D functionals,[8,9] as indicated below, for which analytic Hessians are available for comparison to FD results. The SG-1 quadrature grid[10] was used for all calculations. Geometries were optimized subject to convergence thresholds (in atomic units) of 1.0×10^{-6}, 1.2×10^{-3}, and 3.0×10^{-4} on the stepwise energy difference, the stepwise atomic displacement, and

K.-Y. Liu, J. Liu, J. M. Herbert
Department of Chemistry and Biochemistry, The Ohio State University, Columbus, Ohio 43210 E-mail: herbert@chemistry.ohio-state.edu
*Present address: Max-Planck-Institut für Kohlenforschung, Mülheim an der Ruhr, Germany

Contract grant sponsor: U.S. Department of Energy, Office of Basic Energy Sciences, Division of Chemical Sciences, Geosciences, and Biosciences; Contract grant number: DE-SC0008550; Contract grant sponsor: the National Science Foundation; Contract grant number: CHE-1300603

Table 1. Analytical frequencies and errors (ΔFD) in the FD result, in cm^{-1}, for the F38 dataset.

	B3LYP/6-311G**		ωB97X-D/aug-cc-pVTZ	
Molecule	Analytical	ΔFD	Analytical	ΔFD
C_2H_2	642.81	−0.01	764.12	−0.02
	642.81	−0.01	764.12	0.01
	773.55	−0.01	855.70	0.02
	773.55	−0.01	855.70	0.04
	2070.11	0.00	2085.36	0.00
	3420.37	−0.01	3421.20	0.02
	3523.31	−0.01	3529.42	0.01
CH_4	1340.04	0.00	1349.56	−0.01
	1341.36	0.00	1376.83	−0.01
	1341.85	0.00	1392.07	0.00
	1559.63	0.00	1585.72	0.00
	1560.26	0.00	1589.53	0.00
	3026.91	0.00	3034.65	−0.02
	3132.41	−0.01	3150.21	0.02
	3132.91	−0.01	3151.16	0.01
	3133.00	−0.01	3159.19	0.01
Cl_2	501.11	0.00	589.28	−0.01
CO_2	666.45	0.00	690.00	−0.01
	666.45	−0.01	690.00	0.00
	1376.38	0.00	1393.89	0.01
	2437.53	0.00	2435.03	0.01
N_2	2448.01	−0.01	2494.88	0.01
N_2O	607.38	−0.01	634.91	−0.01
	607.38	−0.01	634.91	−0.01
	1335.97	0.00	1359.73	0.00
	2356.09	0.00	2397.62	0.01
OH	3700.02	−0.03	3769.58	0.01
CO	2222.51	0.00	2245.50	0.01
F_2	984.85	−0.01	1094.45	0.01
H_2CO	1199.21	0.00	1199.61	0.02
	1270.24	0.01	1242.44	0.01
	1538.71	0.00	1504.97	0.00
	1825.92	−0.01	1841.80	0.01
	2869.79	0.00	2903.22	−0.02
	2919.26	0.00	2968.16	0.00
H_2	4418.58	−0.02	4431.91	0.00
H_2O	1636.14	0.01	1634.53	−0.01
	3814.26	−0.01	3888.69	0.01
	3910.36	−0.01	3996.34	0.01
HCN	787.26	0.00	843.42	−0.03
	787.26	0.00	843.42	0.00
	2201.69	0.01	2228.30	0.00
	3454.67	0.01	3455.38	0.02
HF	4125.36	−0.01	4158.40	0.01
NH_3	1073.31	0.01	1034.35	0.00
	1682.04	0.00	1668.94	−0.01
	1682.74	0.00	1688.55	−0.01
	3457.65	−0.01	3507.31	0.02
	3575.98	−0.01	3632.64	0.02
	3576.60	0.00	3634.94	0.01
Average		0.01		0.01

maximum component of the gradient, respectively. FD calculations were performed using a home-built driver code, FRAGME∩T, originally developed for fragment-based quantum chemistry calculations,[11–15] but which is readily adapted to the present purpose. The FRAGME∩T code is currently interfaced with several quantum chemistry programs including Q-CHEM,[16] GAMESS,[17] PSI4,[18] and NWCHEM;[19] Q-CHEM is used for all of the electronic structure calculations presented here.

Unless stated otherwise, the FD calculations presented herein use the traditional three-point stencil,

$$f''(x_0) = \frac{f'(x_0+h) - f'(x_0-h)}{2h} + \mathcal{O}(h^2)\,, \tag{1}$$

with a step size $h = 0.001$ Å. Here, $f'(x) = \partial E/\partial x$ represents the analytic energy gradient. For nonbonded modes, we also explore the use of a five-point stencil,

$$f''(x_0) = \frac{1}{12h}[-f'(x_0+2h) + 8f'(x_0+h) - 8f'(x_0-h) + f'(x_0-2h)] + \mathcal{O}(h^4)\,. \tag{2}$$

Results and Discussion

Benchmark datasets

We first ask the simple question of how well the FD approach reproduces the vibrational frequencies themselves. We examine this question first using the F38 database of vibrational frequencies,[20] which was designed to include a broad range of vibrational frequencies for small molecules. Individual FD frequencies in Table 1, computed at two different levels of theory, exhibit excellent agreement with analytical frequencies, with mean unsigned errors (MUEs) of only 0.01 cm^{-1} and a maximum error of 0.03 cm^{-1}. Statistical results shown in Figure 1 demonstrate that similar accuracy is obtained in various basis sets and at various levels of theory, with nearly all of the errors being < 0.1 cm^{-1}.

We also examine six of the large noncovalent complexes in the L7 dataset,[21] whose structures are shown in Figure 2 and

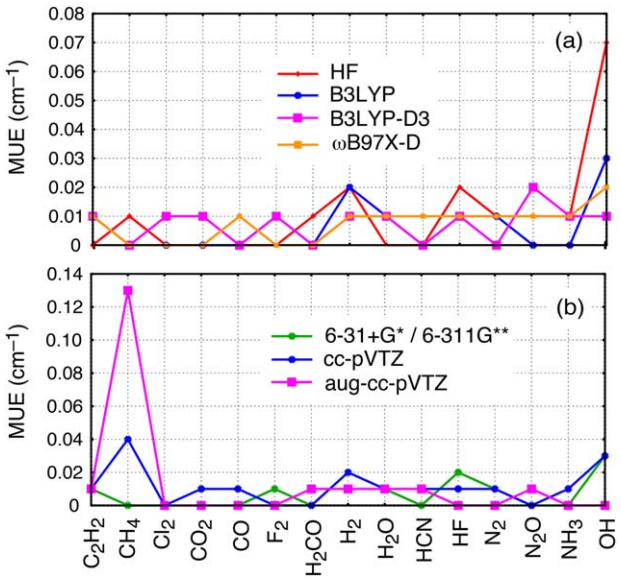

Figure 1. a) MUEs for finite-difference errors for the F38 dataset, averaged across five different theoretical models and all vibrational modes, with all calculations using the 6-311G** basis set. b) MUEs for B3LYP finite-difference frequencies for F38 in various basis sets, averaged across all vibrational modes in each molecule. The 6-31 + G* and 6-311G** results in (b) are indistinguishable on this scale. [Color figure can be viewed at wileyonlinelibrary.com]

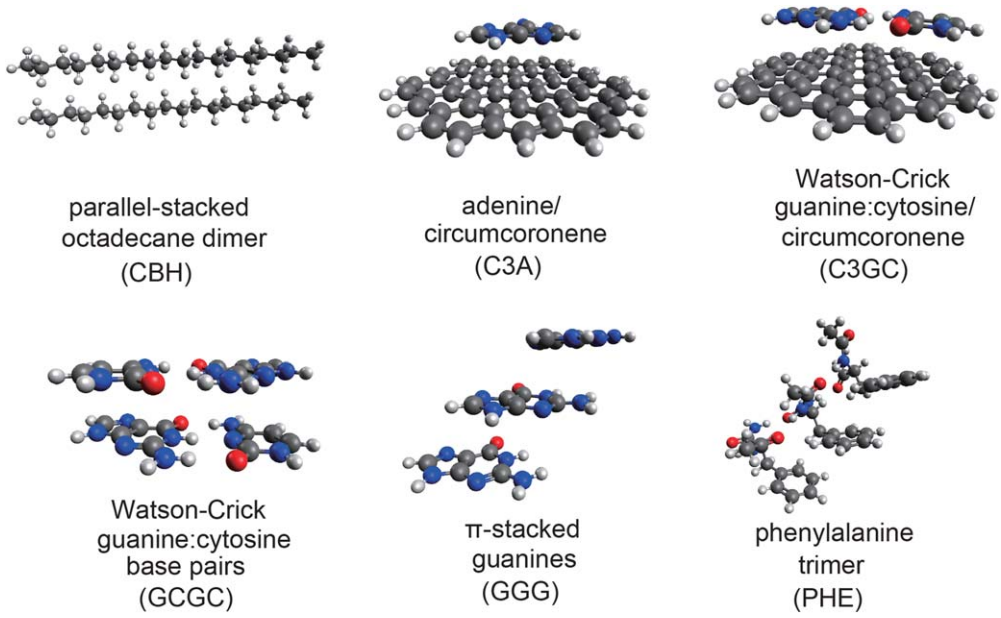

Figure 2. Complexes from the L7 dataset of Ref. [21]. [Color figure can be viewed at wileyonlinelibrary.com]

which are bound primarily by dispersion. (Coordinates for the optimized structures are provided in the Supporting Information.) For such complexes, we expect low-frequency vibrations along intermolecular coordinates, which might be problematic for the FD approach. We compute FD frequencies using the B3LYP/6-311G** and B3LYP-D3/6-31 + G* levels of theory, with overall error statistics for each complex listed in Table 2. Although the MUEs in the FD frequencies, when averaged over all vibrational modes, are small (1–2 cm^{-1}), such averaging hides the larger errors in the low-frequency modes. Maximum errors at the B3LYP-D3/6-31 + G* level range up to 32 cm^{-1} for the C3A and C3GC complexes, corresponding in both cases to a wobbling mode of circumcoronene whose frequency is $\nu = 913$ cm^{-1} (C3A) and $\nu = 1078$ cm^{-1} (G3GC). The distribution of FD errors for two of these complexes can be found in the Supporting Information.

The frequencies quoted above are not *extremely* low, especially for complexes having numerous frequencies below 100 cm^{-1}, and indeed we obtained very accurate FD results for frequencies on the order of ~1000 cm^{-1} in the F38 dataset. Therefore, the large FD errors in these L7 cases must reflect the flatness of the potential energy surface along the nonbonded vibrational modes, and one can reasonably argue that it is inappropriate to apply the harmonic approximation to these sorts of vibrations. This, combined with the accuracy of the FD approach for medium- to high-frequency modes, and its computational advantages in terms of low memory and ease of parallelization, lead us to conclude that the FD approach can be useful even in noncovalent complexes such as these.

In view of the larger FD errors for nonbonded modes, however, we have performed a systematic study of the effects of the FD displacement step size, h, in a more computationally tractable nonbonded system, namely, the parallel-displaced, π-stacked isomer of the benzene dimer. In addition, we test both the three-point and five-point stencil algorithms, eqs. (1) and (2). Results are shown in Table 3. For step sizes $h \leq 0.001$ Å (i.e., equal to or smaller than our default value), the five-point algorithm leaves the maximum FD error unchanged or even slightly increased. Due to the very flat nature of the potential energy surface along the mode in question, however, larger step sizes can be more successful, especially when used

Table 2. Error statistics for finite-difference vibrational frequencies for complexes in the L7 dataset.

	Max. error (cm^{-1})		MUE[b] (cm^{-1})	
Complex[a]	B3LYP/ 6-311G*	B3LYP-D3/ 6-31+G*	B3LYP/ 6-311G*	B3LYP-D3/ 6-31+G*
C3A	4.00	32.43	0.59	2.62
C3GC	7.50	32.26	0.74	2.16
GCGC	−1.07	−4.52	0.07	1.19
GGG	−0.55	4.84	0.03	1.06
CBH	−2.60	−23.97	0.39	1.46
PHE	−2.40	−6.37	0.23	0.33
Average			0.38	1.47

[a] See Fig. 2. [b] Averaged over all vibrational modes.

Table 3. Error statistics in finite-difference vibrational frequencies for the parallel-displaced isomer of $(C_6H_6)_2$ for various finite-difference schemes.

	Max. error (cm^{-1})		MUE[a] (cm^{-1})	
Step size, h (Å)	Three-point[b]	Five-point[c]	Three-point[b]	Five-point[c]
0.0100	3.30	−0.03	0.23	0.01
0.0050	0.90	−0.04	0.05	0.01
0.0010	−1.04	−1.22	0.13	0.17
0.0005	2.17	2.87	0.19	0.20
0.0001	6.63	6.63	0.59	0.59

[a] Averaged over all vibrational modes. [b] Equation (1). [c] Equation (2).

Table 4. Error statistics for finite-difference vibrational frequencies in water clusters.

	Max. error (cm^{-1})		MUE[a] (cm^{-1})	
Cluster	B3LYP/ 6-311G**	ωB97X-D/ aug-cc-pVTZ	B3LYP/ 6-311G**	ωB97X-D/ aug-cc-pVTZ
$(H_2O)_2$	0.03	0.02	0.01	0.01
$(H_2O)_3$	0.01	0.03	0.01	0.01
$(H_2O)_4$	0.04	0.08	0.01	0.02
$(H_2O)_5$	0.05	0.04	0.01	0.01
$(H_2O)_6$ (book)	−0.98	0.03	0.03	0.01
$(H_2O)_6$ (cage)	0.04	0.07	0.01	0.01
$(H_2O)_6$ (prism)	−0.03	0.03	0.01	0.01
$(H_2O)_6$ (ring)	0.24	0.11	0.03	0.02
Average			0.02	0.01

[a] Averaged over all vibrational modes.

with the five-point algorithm. For $h = 0.01$ Å the five-point algorithm reduces the errors to the level obtained for F38, namely, < 0.1 cm^{-1}. Hence, even given the aforementioned caveat regarding the appropriateness of the harmonic approximation for nonbonded modes, it is possible to use the FD approach to reproduce even very small harmonic frequencies.

Conformation-dependent frequency shifts

An important aspect of making contact between *ab initio* frequency calculations and experimental vibrational spectroscopy is the ability to capture the vibrational frequency shifts engendered by conformational changes in a molecule. We examine these here, for water clusters and for conformational isomers of several hydrocarbons. Isomers of a flexible (tryptamine)$\cdots$(H_2O) complex are also considered below in the context of isotopic frequency shifts.

Vibrational frequencies in clusters $(H_2O)_{2\text{-}6}$ have been benchmarked in a previous study using CCSD(T) calculations.[22] The red-shifted hydrogen-bonded O—H stretching vibrations are found to be sensitive to the level of theory, with errors compared to CCSD(T) results that range from nearly zero to more than 100 cm^{-1}. In the present work, we wish to establish whether the FD approach can capture differences in the O—H frequencies for water molecules in different hydrogen-bonding environments. Average errors in *absolute* vibrational frequencies for water clusters are provided in Table 4.

At the level of B3LYP/6-311G**, maximum errors for $(H_2O)_{2\text{-}5}$ are 0.03, 0.01, 0.04, and 0.05 cm^{-1} for $n = 2$, 3, 4, and 5, respectively, and at the ωB97X-D/aug-cc-pVTZ level these maximum errors are 0.02, 0.03, 0.08, and 0.04 cm^{-1}. We also examine four different conformers of $(H_2O)_6$, for which we find no FD error larger than 1 cm^{-1}, and in that particular case, the outlier corresponds to the lowest vibrational frequency (ν=37.71 cm^{-1}) rather than an O–H stretching mode. Average FD errors (Table 4) are 0.02 and 0.01 cm^{-1} for these water clusters.

Given the results for the small-molecule F38 database, it is safe to assume that the FD frequencies for a single H_2O molecule are quite accurate. As such, the FD errors in vibrational frequencies can be taken to be equivalent to the errors in the vibrational red shifts associated with hydrogen bonding. These errors, for the O—H stretching modes, are listed in Table 5 and are < 0.1 cm^{-1}. Errors of such small magnitude imply that the FD approach is capable of distinguishing subtle frequency shifts due to changes in the hydrogen-bonding environment of a particular water molecule.

The 1,2-diphenoxyethane (DPOE) molecule, (C_6H_5)—$O(CH_2)_2$ O—(C_6H_5), is a model of a flexible bi-chromophore whose central aliphatic linkage serves as the repetitive unit of polyethylene and poly(ethylene oxide) polymers. The symmetries of the two most abundant conformational isomers of DPOE were previously determined to be C_2 and C_{2h}.[23] Analytic harmonic frequencies for the modes related to the aforementioned linkage are 1500.09, 1500.38, 1530.97, and 1532.74 cm^{-1} (C_2 symmetry) and 1519.54, 1522.64, 1534.76, and 1535.66 cm^{-1} (C_{2h} symmetry). The FD procedure reproduces not only the frequencies but also

Table 5. Finite-difference errors (in cm^{-1}) for vibrational O—H red shifts in water clusters.

Cluster	B3LYP/ 6-311G**	ωB97X-D/ aug-cc-pVTZ
$(H_2O)_2$	0.01	0.02
$(H_2O)_3$	0.00	0.02
	0.01	0.01
	0.00	0.01
$(H_2O)_4$	0.02	0.01
	0.01	0.03
	0.01	−0.02
	0.01	0.00
$(H_2O)_5$	0.01	−0.01
	0.01	0.01
	0.01	0.01
	0.01	0.00
	0.01	−0.01
$(H_2O)_6$	0.01	0.01
(book)	0.00	0.01
	0.01	0.02
	0.01	0.00
	0.01	0.00
	0.01	0.01
	0.01	0.00
$(H_2O)_6$	0.00	0.01
(cage)	0.01	0.00
	0.00	−0.01
	0.00	−0.01
	0.01	−0.01
$(H_2O)_6$	0.01	0.00
(prism)	0.01	0.01
	0.01	0.00
	0.01	0.00
	0.00	0.01
	0.00	0.01
	0.01	0.00
	0.00	0.00
	0.00	−0.01
$(H_2O)_6$	0.01	0.01
(ring)	−0.06	0.03
	−0.05	0.03
	0.08	0.01
	0.07	0.01
	−0.07	0.11

Table 6. Error statistics for finite-difference calculations of structure-dependent frequency shifts.

	Error (cm^{-1})	
Molecule	max	MUE[a]
DPOE (C_{2h})	0.04	0.01
DPOE (C_2)	0.03	0.01
Ethanethiol (C)	−0.07	0.01
Ethanethiol (G)	−0.02	0.01
Ethanethiol (S)	−0.01	0.01
Ethanethiol (T)	−0.01	0.01

[a] Averaged over vibrational modes.

the frequency *shifts* quite faithfully, with errors in the shifts of only ∼0.01 cm^{-1}; see Table 6.

The cysteine residue's side chain is essential for protein structure due to its flexibility and ability to form disulfide bonds with other cysteine residues. The vibrational spectroscopy of this molecule has been studied, and it is found that the S—H stretching frequency is quite sensitive to hydrogen bonding.[24] As a model system to study this effect, we selected conformational isomers of ethanethiol that are classified by the C^{α}—C^{β}—S—H dihedral angel: two local minima with angles of ∼60° (G isomer) and ∼180° (T isomer), and structures that represent local maxima along the torsional potential, with the angles of ∼0° (C isomer) and ∼120° (S isomer). Analytic frequencies ν_{SH} are 2832.26, 2696.91, 2826.27, and 2831.07 cm^{-1} for isomers G, T, C, and S, respectively. FD errors are again $\leq$ 0.01 cm^{-1} (Table 6), much smaller than the resolution needed to distinguish between these isomers using vibrational spectroscopy.

Isotopic shifts

Isotopic substitution is an important means of assigning experimental vibrational spectra. The (tryptamine)···(H_2O) complex depicted in Figure 3 provides an example that has conformational flexibility, with at least two conformers that are spectroscopically accessible in the gas phase, and isotopic frequency shifts (replacing H_2O with D_2O) have been measured.[25] The O–H stretching frequencies ν_1 and ν_2 are listed in Table 7, and shift from 3474.91 and 3491.04 cm^{-1} to 2553.44 and 2823.69 cm^{-1} upon deuteration (B3LYP/6-311G** level). Errors in the FD calculation of the isotopic frequency *shift* are a mere 0.01 cm^{-1} (ν_1) and 0.04 cm^{-1} (ν_2), at the level of B3LYP/6-311G**. The corresponding errors at the ωB97X-D/6-31 + G* level are −0.03 and −0.02 cm^{-1}.

Table 7. Errors (in cm^{-1}) in selected isotopic shifts.

System	B3LYP/ 6-311G**	ωB97X-D/ 6-31+G*
tryptamine + H_2O[a]		
ν_1	0.01	−0.03
ν_2	0.04	−0.02
1,4,6,9-TCDD[b]		
ν_1	−0.01	−0.01
ν_2	−0.01	−0.01
2,3,7,8-TCDD[b]		
ν_1	0.00	0.01
SF_6[c]		
ν_3	0.00	0.00
ν_4	0.01	0.00

[a] H_2O to D_2O. [b] ^{35}Cl to ^{37}Cl. [c] ^{32}S to ^{34}S.

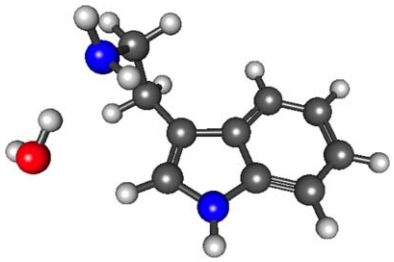

Figure 3. The (tryptamine)···(H_2O) complex of Ref. [25]. [Color figure can be viewed at wileyonlinelibrary.com]

In contrast to the rather large frequency shifts on deuteration, isotopic shifts for ^{35}Cl versus ^{37}Cl in tetrachlorodibenzo-*p*-dioxins (TCDDs, Figure 4) amount to a mere 1–2 cm^{-1} in some cases.[26] The frequencies themselves, corresponding to stretching modes involving Cl, are also much smaller, and shift from 330.14 and 331.63 cm^{-1} to 322.13 and 323.46 cm^{-1} in the case of 1,4,6,9-TCDD (B3LYP/6-311G** level). In 2,3,7,8-TCDD, there is only one mode that is clearly a C—Cl stretch is both isotopologues; this mode shifts from 328.36 to 322.76 cm^{-1} upon isotopic substitution. Despite these rather small shifts, the FD error in the calculated frequency shift is $\leq$ 0.01 cm^{-1} in magnitude for both molecules (see Table 7), such that the shift is clearly resolvable in the FD calculation.

Finally, high-resolution gas-phase spectra of SF_6 reveal isotopic shifts in the ν_3 and ν_4 fundamentals that range from a few

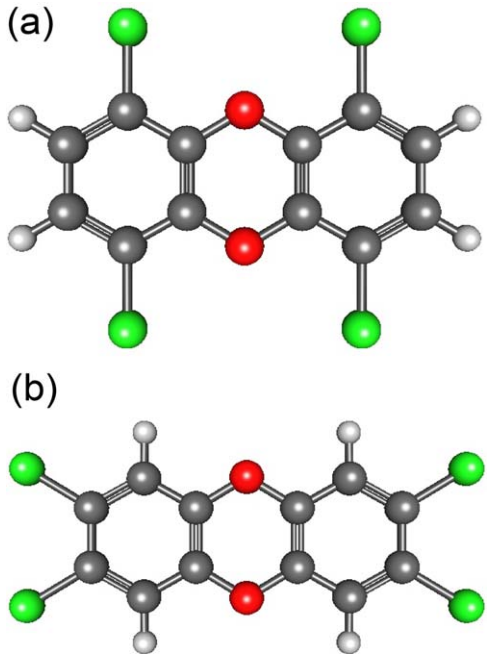

Figure 4. a) 1,4,6,9-TCDD and b) 2,3,7,8-TCDD. [Color figure can be viewed at wileyonlinelibrary.com]

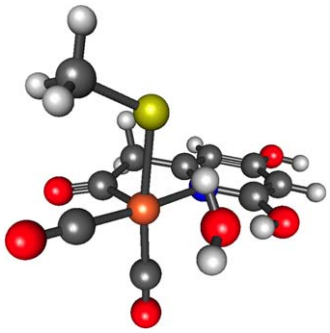

Figure 5. Model of the Hmd active site in its resting state, Hmd—H_2O, from Ref. [28]. [Color figure can be viewed at wileyonlinelibrary.com]

Table 8. Error statistics for finite-difference harmonic frequencies in a model of the Hmd active site.[a]

	Error (cm^{-1})	
System	max	MUE[b]
Hmd—H_2O	0.20	0.05
Hmd—$H_2O + H^+$	0.65	0.06
Hmd—CO	0.40	0.04
Hmd—$CO + H^+$	0.42	0.05

[a] B3LYP/cc-pVTZ level, with *g* functions removed from Fe. [b] Averaged over vibrational modes.

cm^{-1} up to 17 cm^{-1}.[27] Calculated isotopic shifts agree well: −2.26 and −17.11 cm^{-1}. FD errors (Table 7) are $\leq$ 0.01 cm^{-1}.

Hydrogenase active site model

Hydrogenase enzymes have attracted much attention because they use an H_2-based energy cycle rather than a CO_2-based cycle. Recently, a model of 5,10-methenyltetrahydromethanopterin hydrogenase (Hmd) has been studied with density functional theory (see Figure 5),[28] with the results suggesting that charge transfer from Fe 3d orbitals into unoccupied orbitals can lead to variations in the observed C≡O stretching frequencies. The ligand binding process is coupled with protonation of a thiolate ligand, hence protonated structures were included in our analysis. Harmonic frequencies are computed at the B3LYP/cc-VTZ level of theory, but with *g* functions removed from Fe.

Errors in the two C≡O stretching frequencies are both 0.03 cm^{-1} for the resting state (Hmd—H_2O), and are 0.05 and 0.04 cm^{-1} for the protonated state. For Hmd—CO, errors in the three C≡O stretching modes are 0.01, 0.02, and 0.00 cm^{-1}, and for the protonated species (Hmd—$CO + H^+$) they are 0.01, 0.01, and 0.06 cm^{-1}. Although the C≡O modes are the primary ones of experimental interest, error statistics for all frequencies of the model system in Figure 5 are listed in Table 8. None of the errors exceed 0.65 cm^{-1}.

Conclusion

The finite-difference approach to harmonic frequencies was studied at the level of DFT, in the interest of obtaining a highly parallelizable, low-memory approach that does not require derivation and implementation of analytic second derivatives. Perhaps contrary to established conventional wisdom, we find that finite-difference results differ from those obtained using an analytic Hessian by < 0.1 cm^{-1} in most cases. Even frequencies in the 500–1000 cm^{-1} range are accurately reproduced, as are frequency shifts arising either from conformational changes or isotopic substitution. Vibrational red-shifts in the O—H stretching modes of water clusters, due to changes in the hydrogen-bonding environment, are also accurately reproduced by the finite-difference approach. The only significant errors that we find are in low-frequency nonbonded modes in dispersion-bound complexes, where the potential surface is very flat. In these cases, our "standard" finite-difference approach, based on displacements of ±0.001 Å, results in errors as large as 32 cm^{-1}, but can be reduced to < 0.1 cm^{-1} by appropriate choice of the displacement in conjunction with a five-point stencil that are requires four energy gradient calculations per degree of freedom.

In view of their accuracy, easy parallelizability and low memory footprint, we see no reason not to recommend the finite-difference approach to DFT harmonic frequency calculations. This should extend harmonic analysis to cases where analytic Hessian calculations are cumbersome, intractable, or where the Hessian simply has not been implemented.

Acknowledgments

Calculations were performed at the Ohio Supercomputer Center under project no. PAA-0003.[29] *J.M.H. is a fellow of the Alexander von Humboldt Foundation.*

Keywords: finite difference · harmonic frequencies · isotopic shifts · noncovalent interactions · density functional theory

How to cite this article: K.-Y. Liu, J. Liu, J. M. Herbert. *J. Comput. Chem.* **2017**, *38*, 1678–1684. DOI: 10.1002/jcc.24811

Additional Supporting Information may be found in the online version of this article.

[1] J. A. Pople, R. Krishnan, H. B. Schegel, J. S. Binkley, *Int. J. Quantum Chem. Symp.* **1979**, *13*, 225.
[2] P. P. Korambath, J. Kong, T. R. Furlani, M. Head-Gordon, *Mol. Phys.* **2002**, *100*, 1771.
[3] O. V. Vydrov, T. van Voorhis, *J. Chem. Phys.* **2010**, *133*, 244103.
[4] N. Mardirossian, M. Head-Gordon, *Phys. Chem. Chem. Phys.* **2014**, *16*, 9904.
[5] N. Mardirossian, M. Head-Gordon, *J. Chem. Phys.* **2015**, *142*, 074111.
[6] N. Mardirossian, M. Head-Gordon, *J. Chem. Phys.* **2016**, *144*, 214110.
[7] S. Grimme, J. Antony, S. Ehrlich, H. Krieg, *J. Chem. Phys.* **2010**, *132*, 154104.
[8] J.-D. Chai, M. Head-Gordon, *J. Chem. Phys.* **2008**, *128*, 084106.
[9] J.-D. Chai, M. Head-Gordon, *Phys. Chem. Chem. Phys.* **2008**, *10*, 6615.
[10] P. M. W. Gill, B. G. Johnson, J. A. Pople, *Chem. Phys. Lett.* **1993**, *209*, 506.
[11] R. M. Richard, J. M. Herbert, *J. Chem. Phys.* **2012**, *137*, 064113.
[12] R. M. Richard, J. M. Herbert, *J. Chem. Theory Comput.* **2013**, *9*, 1408.
[13] R. M. Richard, K. U. Lao, J. M. Herbert, *J. Chem. Phys.* **2014**, *141*, 014108.

[14] K. U. Lao, K.-Y. Liu, R. M. Richard, J. M. Herbert, *J. Chem. Phys.* **2016**, *144*, 164105.
[15] J. Liu, J. M. Herbert, *J. Chem. Theory Comput.* **2016**, *12*, 572.
[16] Y. Shao, Z. Gan, E. Epifanovsky, A. T. B. Gilbert, M. Wormit, J. Kussmann, A. W. Lange, A. Behn, J. Deng, X. Feng, D. Ghosh, M. Goldey, P. R. Horn, L. D. Jacobson, I. Kaliman, R. Z. Khaliullin, T. Kús, A. Landau, J. Liu, E. I. Proynov, Y. M. Rhee, R. M. Richard, M. A. Rohrdanz, R. P. Steele, E. J. Sundstrom, H. L. Woodcock, III, P. M. Zimmerman, D. Zuev, B. Albrecht, E. Alguire, B. Austin, G. J. O. Beran, Y. A. Bernard, E. Berquist, K. Brandhorst, K. B. Bravaya, S. T. Brown, D. Casanova, C.-M. Chang, Y. Chen, S. H. Chien, K. D. Closser, D. L. Crittenden, M. Diedenhofen, R. A. DiStasio, Jr., H. Do, A. D. Dutoi, R. G. Edgar, S. Fatehi, L. Fusti-Molnar, A. Ghysels, A. Golubeva-Zadorozhnaya, J. Gomes, M. W. D. Hanson-Heine, P. H. P. Harbach, A. W. Hauser, E. G. Hohenstein, Z. C. Holden, T.- C. Jagau, H. Ji, B. Kaduk, K. Khistyaev, J. Kim, J. Kim, R. A. King, P. Klunzinger, D. Kosenkov, T. Kowalczyk, C. M. Krauter, K. U. Lao, A. Laurent, K. V. Lawler, S. V. Levchenko, C. Y. Lin, F. Liu, E. Livshits, R. C. Lochan, A. Luenser, P. Manohar, S. F. Manzer, S.- P. Mao, N. Mardirossian, A. V. Marenich, S. A. Maurer, N. J. Mayhall, C. M. Oana, R. Olivares-Amaya, D. P. O'Neill, J. A. Parkhill, T. M. Perrine, R. Peverati, P. A. Pieniazek, A. Prociuk, D. R. Rehn, E. Rosta, N. J. Russ, N. Sergueev, S. M. Sharada, S. Sharma, D. W. Small, A. Sodt, T. Stein, D. Stück, Y.-C. Su, A. J. W. Thom, T. Tsuchimochi, L. Vogt, O. Vydrov, T. Wang, M. A. Watson, J. Wenzel, A. White, C. F. Williams, V. Vanovschi, S. Yeganeh, S. R. Yost, Z.-Q. You, I.-Y. Zhang, X. Zhang, Y. Zhao, B. R. Brooks, G. K. L. Chan, D. M. Chipman, C. J. Cramer, I. I. I. W. A. Goddard, M. S. Gordon, W. J. Hehre, A. Klamt, H. F. Schaefer, III, M. W. Schmidt, C. D. Sherrill, D. G. Truhlar, A. Warshel, X. Xu, A. Aspuru-Guzik, R. Baer, A. T. Bell, N. A. Besley, J.- D. Chai, A. Dreuw, B. D. Dunietz, T. R. Furlani, S. R. Gwaltney, C.- P. Hsu, Y. Jung, J. Kong, D. S. Lambrecht, W. Liang, C. Ochsenfeld, V. A. Rassolov, L. V. Slipchenko, J. E. Subotnik, T. Van Voorhis, J. M. Herbert, A. I. Krylov, P. M. W. Gill, M. Head-Gordon, *Mol. Phys.* **2015**, *113*, 184.
[17] M. W. Schmidt, K. K. Baldridge, J. A. Boatz, S. T. Elbert, M. S. Gordon, J. H. Jensen, S. Koseki, N. Matsunaga, K. A. Nguyen, S. Su, T. L. Windus, M. Dupuis, J. A. Montgomery, Jr., *J. Comput. Chem.* **1993**, *14*, 1347.
[18] J. M. Turney, A. C. Simmonett, R. M. Parrish, E. G. Hohenstein, F. Evangelista, J. T. Fermann, B. J. Mintz, L. A. Burns, J. J. Wilke, M. L. Abrams, N. J. Russ, M. L. Leininger, C. L. Janssen, E. T. Seidl, W. D. Allen, H. F. Schaefer, R. A. King, E. F. Valeev, C. D. Sherrill, T. D. Crawford, *WIREs Comput. Mol. Sci.* **2012**, *2*, 556.
[19] M. Valiev, E. J. Bylaska, N. Govind, K. Kowalski, T. P. Straatsma, H. J. J. van Dam, D. Wang, J. Nieplocha, E. Apra, T. L. Windus, W. A. de Jong, *Comput. Phys. Commun.* **2010**, *181*, 1477.
[20] Y. Zhao, D. G. Truhlar, *Theor. Chem. Acc.* **2008**, *120*, 215.
[21] R. Sedlak, T. Janowski, M. Pitoňák, J. Řezáč, P. Pulay, P. Hobza, *J. Chem. Theory Comput.* **2013**, *9*, 3364.
[22] J. C. Howard, G. S. Tschumper, *J. Chem. Theory Comput.* **2015**, *11*, 2126.
[23] E. G. Buchanan, E. L. Sibert, T. S. Zwier, *J. Phys. Chem. A* **2013**, *117*, 2800.
[24] W. L. Qian, S. Krimm, *Biopolymers* **1992**, *32*, 1503.
[25] J. R. Clarkson, J. M. Herbert, T. S. Zwier, *J. Chem. Phys.* **2007**, *126*, 134306:1.
[26] G. Rauhut, P. Pulay, *J. Am. Chem. Soc.* **1995**, *117*, 4167.
[27] T. D. Kolomiitsova, V. A. Kondaurov, E. V. Sedelkova, D. N. Shchepkin, *Opt. Spectrosc.* **2002**, *92*, 512.
[28] A. Dey, *J. Am. Chem. Soc.* **2010**, *132*, 13892.
[29] Ohio Supercomputer Center. Available at: http://osc.edu/ark:/19495/f5s1ph73

Received: 24 January 2017
Accepted: 19 March 2017
Published online on 10 May 2017